

# Conditioning Score-Based Generative Models by Neuro-Symbolic Constraints

Davide Scassola<sup>1,2</sup>, Sebastiano Sacconi<sup>2</sup>, Ginevra Carbone<sup>2</sup>, Luca Bortolussi<sup>1</sup>

<sup>1</sup>AILAB, University of Trieste, Trieste, Italy

<sup>2</sup>Aindo, AREA Science Park, Trieste, Italy

davide.scassola@phd.units.it, sebastiano@aindo.com, ginevra@aindo.com, lbortolussi@units.it

## Abstract

Score-based and diffusion models have emerged as effective approaches for both conditional and unconditional generation. Still conditional generation is based on either a specific training of a conditional model or classifier guidance, which requires training a noise-dependent classifier, even when the classifier for uncorrupted data is given. We propose an approach to sample from unconditional score-based generative models enforcing arbitrary logical constraints, without any additional training. Firstly, we show how to manipulate the learned score in order to sample from an un-normalized distribution conditional on a user-defined constraint. Then, we define a flexible and numerically stable neuro-symbolic framework for encoding soft logical constraints. Combining these two ingredients we obtain a general, but approximate, conditional sampling algorithm. We further developed effective heuristics aimed at improving the approximation. Finally, we show the effectiveness of our approach for various types of constraints and data: tabular data, images and time series.

## Introduction

Score-based (Song and Ermon 2019) and diffusion (Ho, Jain, and Abbeel 2020; Sohl-Dickstein et al. 2015) generative models based on deep neural networks have proven effective in modelling complex high-dimensional distributions in various domains. Controlling these models in order to obtain desirable features in samples is often required, still most conditional models require additional constraint-specific training in order to perform conditional sampling. As with most generative models, one can directly train a conditional generative model. Score-based and diffusion models offer the alternative of separately training an unconditional model and a noise-conditional classifier, whose gradient is used to guide the reverse diffusion process during sampling (Dhariwal and Nichol 2021). This represents a limit since either one needs to train an extremely flexible conditional model (as those based on text prompts), or alternatively to train a conditional model for any specific constraint to be enforced. Moreover, these conditional models often lack robustness, since the constraint is only learned through labelled data, even when the constraint is a user-defined function.

As a consequence, generating samples that obey some arbitrary but formally specified logical constraints is currently hard. This would be useful in different contexts:

- *Tabular data*: generation of entries that obey formal requirements described by logical formulas, without a specific training for every formula.
- *Surrogate models*: using unconditional surrogate models to efficiently sample imposing physical constraints, or exploring scenarios defined by additional constraints.
- *Image generation*: controlling image generation conditioning on formally specified visual features.

Text prompt conditioned image generation with diffusion models (Rombach et al. 2022) has proven extremely flexible and effective, still it lacks fine grained control and requires a massive amount of labelled samples. Imposing user-defined constraints can alternatively be performed by manipulating the loss function of the generator (regularization), but in this way a specific training is required for any constraint. More recent work focuses on general methods to perform guided diffusion on images, without the need to retrain a noise-dependent classifier (Bansal et al. 2023; Graikos et al. 2022; Kadkhodaie and Simoncelli 2021).

In this article we develop a method for sampling from unconditional score-based generative models, enforcing arbitrary user-defined logical constraints, that does not require additional training. Despite being originally designed for tabular data, we show the application of our method to other types of data. In summary, we present the following key contributions:

- We develop a simple method for applying constraints to unconditional score-based generative models at inference time. The method enables sampling approximately from the product of the learned unconditional distribution and a given un-normalized distribution.
- We define a general neuro-symbolic language for building soft constraints that corresponds to logical formulas. Our framework generates constraints that are numerically stable, satisfy convenient logical properties, and can be relaxed/hardened arbitrarily through a control parameter.
- We test our method on different types of datasets and constraints, showing both good performance on approximating conditional distributions on tabular data, and good quality of samples for high dimensional data such as images and time-series.

## Background

### Score-based generative models

Score-based generative models (Song and Ermon 2019; Song et al. 2021), are a class of models developed in recent years, closely related to diffusion probabilistic models (Sohl-Dickstein et al. 2015; Ho, Jain, and Abbeel 2020). Given the objective to sample from the distribution  $p(\mathbf{x})$  that generated the data, these models aim at estimating the (Stein) score of  $p(\mathbf{x})$ , defined as  $\mathbf{s}(\mathbf{x}) := \nabla_{\mathbf{x}} \ln p(\mathbf{x})$  and then use sampling techniques that exploit the knowledge of the score of the distribution. There are several methods for estimating the score: score matching (Hyvärinen and Dayan 2005), sliced score matching (Song et al. 2020), and denoising score matching (Vincent 2011). Denoising score matching is probably the most popular one, it uses corrupted data samples  $\tilde{\mathbf{x}}$  in order to estimate the score of the distribution for different levels of added noise, which is in practice necessary for sampling in high dimensional spaces (Song and Ermon 2019).

Given a neural network  $\mathbf{s}_{\theta}(\mathbf{x}, t)$  and a diffusion process  $q_t(\tilde{\mathbf{x}}|\mathbf{x})$  defined for  $t \in [0, 1]$  such that  $q_0(\tilde{\mathbf{x}}|\mathbf{x}) \approx \delta(\mathbf{x})$  (no corruption) and  $q_1(\tilde{\mathbf{x}}|\mathbf{x})$  is a fixed prior distribution (e.g., a Gaussian), the denoising score matching loss is:

$$\mathbb{E}_{t \sim u(0,1), \mathbf{x} \sim p(\mathbf{x}), \tilde{\mathbf{x}} \sim q_t(\tilde{\mathbf{x}}|\mathbf{x})} \|\mathbf{s}_{\theta}(\tilde{\mathbf{x}}, t) - \nabla_{\tilde{\mathbf{x}}} \ln q_t(\tilde{\mathbf{x}}|\mathbf{x})\|_2^2$$

With sufficient data and model capacity, denoising score matching ensures  $\mathbf{s}_{\theta}(\mathbf{x}, t) \approx \nabla_{\mathbf{x}} \ln p_t(\mathbf{x})$  for almost all  $\mathbf{x}$  and  $t$ , where  $p_t(\mathbf{x}) := \int q_t(\mathbf{x}|\mathbf{x}_0)p_0(\mathbf{x}_0)d\mathbf{x}_0$  is the distribution of the data for different levels of added noise. Given the estimate of the time/noise dependent score  $\mathbf{s}_{\theta}(\mathbf{x}, t)$ , one can resort to different techniques for sampling from  $p(\mathbf{x}) = p_0(\mathbf{x})$  as annealed Langevin dynamics (Song and Ermon 2019), denoising diffusion probabilistic models or stochastic differential equations (Song et al. 2021), a generalization of the aforementioned approaches.

### Conditional sampling with score-based models

Given a joint distribution  $p(\mathbf{x}, \mathbf{y})$ , one is often interested in sampling from the conditional distribution  $p(\mathbf{x}|\mathbf{y})$ , where  $\mathbf{y}$  is for example a label. While it is possible to directly model the conditional distribution (as usually done in many generative models), in this case by estimating  $\nabla_{\mathbf{x}} \ln p_t(\mathbf{x}|\mathbf{y})$ , score-based generative models allow conditional sampling without explicit training of the conditional generative model. Applying the Bayesian rule  $p_t(\mathbf{x}|\mathbf{y}) = \frac{p_t(\mathbf{y}|\mathbf{x})p_t(\mathbf{x})}{p_t(\mathbf{y})}$  one can observe that:

$$\nabla_{\mathbf{x}} \ln p_t(\mathbf{x}|\mathbf{y}) = \nabla_{\mathbf{x}} \ln p_t(\mathbf{x}) + \nabla_{\mathbf{x}} \ln p_t(\mathbf{y}|\mathbf{x})$$

It follows that one can obtain the conditional score from the unconditional score by separately training a noise-dependent classifier  $p_t(\mathbf{y}|\mathbf{x})$ . This technique is known as ‘‘guidance’’, and it has been used for class conditional image generation (Dhariwal and Nichol 2021).

## Method

### Problem formalization

Given a set of observed samples  $\mathbf{x}_i \in \mathbb{R}^d$ , the goal is to sample from the distribution  $p(\mathbf{x})$  that generated  $\mathbf{x}_i$  conditioning

on a desired property. Let  $\pi(\mathbf{x}) : \mathbb{R}^d \rightarrow \{0, 1\}$  be the function that encodes this property, such that  $\pi(\mathbf{x}) = 1$  when the property is satisfied and  $\pi(\mathbf{x}) = 0$  otherwise. Then the target conditional distribution can be defined as:

$$p(\mathbf{x}|\pi) \propto p(\mathbf{x})\pi(\mathbf{x})$$

Alternatively, one can also define soft constraints, expressing the degree of satisfaction as a real number. Let  $c(\mathbf{x}) : \mathbb{R}^d \rightarrow \mathbb{R}$  be a differentiable function expressing this soft constraint. In this case we define the target distribution as:

$$p^c(\mathbf{x}) \propto p(\mathbf{x})e^{c(\mathbf{x})}$$

It can be shown that  $p^c$  is the distribution that maximizes  $\mathbb{E}_{p^c}[c(\mathbf{x})] - D_{KL}(p^c||p)$  (Hu et al. 2018; Ganchev et al. 2010). Moreover, since the form is analogous to the previous formulation, given a hard constraint  $\pi(\mathbf{x})$  one can build a soft constraint  $c(\mathbf{x})$  such that  $p^c(\mathbf{x}) \approx p(\mathbf{x}|\pi)$ . We then consider  $p^c(\mathbf{x})$  as the target distribution we want to sample from.

### Constraint-based guidance

Our method exploits score-based generative models as the base generative model. As previously introduced, a stochastic process that gradually adds noise to original data  $q(\tilde{\mathbf{x}}|\mathbf{x})$  is defined such that at  $t = 0$  little or no noise is added so  $X_0 \sim p(\mathbf{x})$  and at  $t = 1$  the maximum amount of noise is added such that  $X_1 \sim q_1(\tilde{\mathbf{x}}|\mathbf{x})$  is a known prior distribution (for example a Gaussian). Given the possibility to efficiently sample from  $p_t(\mathbf{x})$ , the time-dependent (Stein) score of  $p_t(\mathbf{x})$  is estimated by score matching using a neural network, let it be  $\mathbf{s}(\mathbf{x}, t) \approx \nabla_{\mathbf{x}} \ln p_t(\mathbf{x})$ . As discussed in the previous section, there are different possible sampling schemes once the score is available. Given the target distribution

$$p^c(\mathbf{x}) := \frac{p(\mathbf{x})e^{c(\mathbf{x})}}{Z}$$

where  $Z$  is the unknown normalization constant, and the distribution of samples from  $p^c(\mathbf{x})$  that are successively corrupted by  $q(\tilde{\mathbf{x}}|\mathbf{x})$ :

$$p_t^c(\mathbf{x}) := \int q_t(\mathbf{x}|\mathbf{x}_0)p^c(\mathbf{x}_0)d\mathbf{x}_0$$

we observe the following relationship:

$$\begin{aligned} \nabla_{\mathbf{x}} \ln p_0^c(\mathbf{x}) &= \nabla_{\mathbf{x}} \ln p^c(\mathbf{x}) = \nabla_{\mathbf{x}} \ln \frac{p(\mathbf{x})e^{c(\mathbf{x})}}{Z} \\ &= \nabla_{\mathbf{x}} [\ln p(\mathbf{x}) + c(\mathbf{x}) - \ln Z] = \nabla_{\mathbf{x}} \ln p(\mathbf{x}) + \nabla_{\mathbf{x}} c(\mathbf{x}) \end{aligned}$$

It follows that at  $t = 0$  one can easily obtain an estimate of the score by summing the gradient of the constraint to the estimate of the score of the unconstrained distribution. Notice that this is possible since taking the gradient of the logarithm eliminates the intractable integration constant  $Z$ . At  $t = 1$  instead one can assume  $\nabla_{\mathbf{x}} \ln p_1^c(\mathbf{x}) = \nabla_{\mathbf{x}} \ln p_1(\mathbf{x})$ , since we assume enough noise is added to make samples from  $p_1^c(\mathbf{x})$  distributed as the prior. In general there is no analytical form for  $\nabla_{\mathbf{x}} \ln p_t^c(\mathbf{x})$ , also, it cannot be estimated by score matching since we are not assuming samples from  $p_0^c(\mathbf{x})$  are available in the first place.

## Conditional score approximation

Given this limit, we resort to approximations  $\tilde{s}_c(\mathbf{x}, t)$  for  $s_c(\mathbf{x}, t) = \nabla_{\mathbf{x}} \ln p_t^c(\mathbf{x})$ . The approximations we use are constructed knowing the true value of the score for  $t = 0$  and  $t = 1$ :

$$\begin{aligned}\tilde{s}_c(\mathbf{x}, 0) &= s(\mathbf{x}, 0) + \nabla_{\mathbf{x}} c(\mathbf{x}) \\ \tilde{s}_c(\mathbf{x}, 1) &= s(\mathbf{x}, 1)\end{aligned}$$

A simple way to obtain this is by weighting the contribution of the gradient of the constraint depending on time:

$$\tilde{s}_c(\mathbf{x}, t) = s(\mathbf{x}, t) + g(t) \nabla_{\mathbf{x}} c(\mathbf{x})$$

where  $g(t) : [0, 1] \rightarrow [0, 1]$  satisfies  $g(0) = 1$  and  $g(1) = 0$ . Sampling from the target distribution then reduces to substituting the score of the base model with the modified score  $\tilde{s}_c(\mathbf{x}, t)$ . Notice that this approach does not require any re-training of the model.

**Langevin MCMC correction.** Depending on the type of data, we found it useful to perform additional Langevin dynamics steps (these are referred to as ‘‘corrector steps’’ in (Song et al. 2021)) at time  $t \approx 0$  when the score of the constrained target distribution is known without approximation. Langevin dynamics can be used as a Monte Carlo method for sampling from a distribution when only the score is known (Parisi 1981), performing the following update, where  $\epsilon$  is the step size and  $\mathbf{z}^i$  is sampled from a standard normal with the dimensionality of  $\mathbf{x}$ :

$$\mathbf{x}^{i+1} = \mathbf{x}^i + \epsilon \tilde{s}_c(\mathbf{x}, 0) + \mathbf{z}^i \sqrt{2\epsilon}$$

In the limit  $i \rightarrow \infty$  and  $\epsilon \rightarrow 0$  Langevin dynamics samples from  $p^c(\mathbf{x})$ . Nevertheless, as most Monte Carlo techniques, Langevin dynamics struggles in exploring all the modes when the target distribution is highly multimodal.

Algorithm 1 summarizes the modified sampling algorithm.

**Choice of score approximation scheme.** We observed the results to be sensitive to the choice of the approximation scheme for  $\nabla_{\mathbf{x}} \ln p_t^c(\mathbf{x})$ . One should choose a  $g(t)$  that is strong enough to guide samples towards the modes of  $p_0^c(\mathbf{x})$  but at the same time that does not disrupt the reverse diffusion process in the early steps. We experimented with various forms of  $g(t)$ , mostly with the following two functions:

- **Linear:**  $g(t) = 1 - t$
- **SNR:**  $g(t)$  is equal to the signal-to-noise ratio of the diffusion kernel. For example, if the diffusion kernel  $q_t(\tilde{\mathbf{x}}|\mathbf{x})$  is  $\mathcal{N}(\mathbf{x}, \sigma_t)$ , then  $g(t) = (1 + \sigma_t^2)^{-\frac{1}{2}}$ , assuming normalized data.

In many of our experiments we found **SNR** to be the most effective, so we suggest using it as the first choice.

## Neuro-Symbolic logical constraints

We will consider a general class of constraints expressed in a logical form. Hard logical constraints cannot be directly used in the approach presented above, hence we turn them into differentiable soft constraints leveraging neuro-symbolic ideas (Badreddine et al. 2020). More specifically,

## Algorithm 1: Constraint guidance sampling

---

**Input:** constraint  $c(\mathbf{x})$ , score  $s(\mathbf{x}, t)$ , score-based sampling algorithm  $A(s)$   
**Parameters:**  $g(t)$ ,  $\epsilon$ ,  $n$   
 $\tilde{s}_c(\mathbf{x}, t) \leftarrow s(\mathbf{x}, t) + g(t) \nabla_{\mathbf{x}} c(\mathbf{x})$   
 $\mathbf{x} \leftarrow A(\tilde{s}_c)$   
**for**  $i = 1$  **to**  $n$  **do**  
     $\mathbf{z} \leftarrow \mathcal{N}(0, 1)$  (with the dimensionality of  $\mathbf{x}$ )  
     $\mathbf{x} \leftarrow \mathbf{x} + \epsilon \tilde{s}_c(\mathbf{x}, 0) + \mathbf{z} \sqrt{2\epsilon}$   
**end for**  
**return**  $\mathbf{x}$

---

we consider predicates and formulae defined on the individual features  $\mathbf{x} = (x_1, \dots, x_d)$  of the data points we ought to generate. Given a Boolean property  $P(\mathbf{x})$  (i.e. a predicate or a formula), with features  $\mathbf{x}$  as free variables, we associate with it a constraint function  $c(\mathbf{x})$  such that  $e^{c(\mathbf{x})}$  approximates the corresponding non-differentiable hard constraint  $\mathbf{1}_{P(\mathbf{x})}$ .<sup>1</sup> In this paper, we consider constraints that can be evaluated on a single or on a few data points, hence we can restrict ourselves to the quantifier-free fragment of first-order logic. Therefore, we can define by structural recursion the constraint  $c(\mathbf{x})$  for atomic propositions and Boolean connectives. As atomic propositions, we consider here simple equalities and inequalities of the form  $a(\mathbf{x}) \geq b(\mathbf{x})$ ,  $a(\mathbf{x}) \leq b(\mathbf{x})$ ,  $a(\mathbf{x}) = b(\mathbf{x})$ , where  $a$  and  $b$  can be arbitrary differentiable functions of feature variables  $\mathbf{x}$ . Following (Badreddine et al. 2020), we refer to such sets of functions as *real logic*.

In particular, we define the semantics directly in log-probability space, obtaining the **Log-probabilistic logic**. The definitions we adopt are partially in line with those of the newly defined *LogLTN*, see (Badreddine, Serafini, and Spranger 2023), and are reported in Table 1.

**Atomic predicates.** We choose to define the inequality  $a(\mathbf{x}) \geq b(\mathbf{x})$  as  $c(\mathbf{x}) = -\ln(1 + e^{-k(a(\mathbf{x}) - b(\mathbf{x}))})$ , introducing an extra parameter  $k$  that regulates the ‘‘hardness’’ of the constraint. Indeed, in the limit  $k \rightarrow \infty$  one have  $\lim_{k \rightarrow \infty} e^{c(\mathbf{x})} = \mathbf{1}_{a(\mathbf{x}) \geq b(\mathbf{x})}$ . This definition is consistent

<sup>1</sup> $\mathbf{1}_{P(\mathbf{x})}$  is indicator function equal to 1 for each  $\mathbf{x}$  such that  $P(\mathbf{x})$  is true.

Formula	Differentiable function
$c[a(\mathbf{x}) \geq b(\mathbf{x})]$	$-\ln(1 + e^{-k(a(\mathbf{x}) - b(\mathbf{x}))})$
$c[a(\mathbf{x}) \leq b(\mathbf{x})]$	$-\ln(1 + e^{-k(b(\mathbf{x}) - a(\mathbf{x}))})$
$c[a(\mathbf{x}) = b(\mathbf{x})]$	$a(\mathbf{x}) \geq b(\mathbf{x}) \wedge a(\mathbf{x}) \leq b(\mathbf{x})$
$c[a(\mathbf{x}) = b(\mathbf{x})]$	$-(a(\mathbf{x}) - b(\mathbf{x}))^2$
$c[\varphi_1 \wedge \varphi_2]$	$c[\varphi_1] + c[\varphi_2]$
$c[\varphi_1 \vee \varphi_2]$	$\ln(e^{c[\varphi_1]} + e^{c[\varphi_2]} - e^{c[\varphi_1] + c[\varphi_2]})$
$c[\neg \varphi]$	$\ln(1 - e^{c[\varphi]})$

Table 1: Semantic rules of log-probabilistic logic. In the table,  $c[\varphi](\mathbf{x})$  is the soft constraint associated with the formula  $\varphi$ .

with negation but its gradient is nonzero when the condition is satisfied,<sup>2</sup> though this was not creating issues in the experiment for sufficiently large values of  $k$ . Regarding equality, we consider two alternatives. The first formulation is the standard definition based on inequalities, while the second (l2 distance) is more common as a soft constraint and corresponds to a Gaussian kernel. Moreover, the first form of equality has a limited gradient while the second does not.

**Boolean connectives.** The conjunction and the disjunction correspond to the product t-norm and its dual t-conorm (probabilistic sum) (van Krieken, Acar, and van Harmelen 2022) but in logarithmic space. We use the material implication rule to reduce the logical implication to a disjunction:  $a \rightarrow b \equiv \neg a \vee b$ . The negation, instead, is consistent with the semantic definition of inequalities: negating one inequality, one obtains its flipped version. For numerical stability reasons, however, we choose to avoid using the soft negation function in any case. Instead, we reduce logical formulas to the negation normal form (NNF) as in (Badreddine, Serafini, and Spranger 2023), where negation is only applied to atoms, for which the negation can be computed analytically or defined. In order to simplify the notation, in the following we will also use quantifiers ( $\forall$  and  $\exists$ ) as syntactic sugar (in place of conjunctions or disjunctions) only when the quantified variable takes values in a finite and known domain (e.g. time instants in a time series or pixels in an image).

The difference in our definition with respect to *LogLTN* is in the logical disjunction ( $\vee$ ): they define it using the Log-MeanExp (LME) operator, an approximation of the maximum that is numerically stable and suitable for derivation. They do it at the price of losing the possibility to reduce formulas to the NNF exactly (using De Morgan’s laws) that follows from having as disjunction the dual t-conorm of the conjunction. We choose instead to use the log-probabilistic sum as the disjunction since in the domain of our experiments it proved numerically stable and effective.

When sampling, we can regulate the tradeoff between similarity with the original distribution and strength of the constraint by tuning the parameter  $k$  of inequalities in log-probabilistic logic. Alternatively, we can multiply by a constant  $\lambda$  the value of the constraint in order to scale its gradient.

Given the flexibility of this logical framework, we can also perform conditional generation imposing constraints on a batch of samples, by defining formulae with free variables corresponding to features of different samples in the batch, therefore conditioning the joint distribution (which is unconditionally independent). Future work will further explore this possibility.

## Experiments

We test our method on several datasets, all of which have only real-valued features, e.g. with data points in  $\mathbb{R}^d$ .

<sup>2</sup>This can be addressed by defining a simplified version:  $a(\mathbf{x}) \geq b(\mathbf{x}) \equiv k(a(\mathbf{x}) - b(\mathbf{x}))\mathbf{1}_{a(\mathbf{x}) < b(\mathbf{x})}$ , however such a definition will no more be consistent with negation.

The quality evaluation of conditionally generated samples is challenging. First of all, one should compare conditionally generated samples with another method to generate conditionally in an exact way. We chose then to compare our approach with rejection sampling, that can be used to sample exactly from the product of two distributions  $p(\mathbf{x})$  and  $q(\mathbf{x})$ , where sampling from  $p(\mathbf{x})$  is tractable and  $q(\mathbf{x})$  density is known up to a normalization constant. In our case  $p(\mathbf{x})$  is the unconditional generative model and  $q(\mathbf{x}) = e^{c(\mathbf{x})}$ . Assuming constraints are such that  $\forall \mathbf{x} c(\mathbf{x}) \leq 0$ , then  $q(\mathbf{x})$  is upper-bounded by 1. This upper bound is guaranteed by the real logic we defined previously. Rejection sampling then reduces to sampling from  $p(\mathbf{x})$  and accepting each sample with probability  $q(\mathbf{x})$ . This can be problematic when the probability of a random sample from  $p(\mathbf{x})$  having a non-null value of  $q(\mathbf{x})$  is low.

In the second place, comparing the similarity of two samples is a notoriously difficult problem. For relatively low dimensional samples, we will compare the marginal distributions and the correlation matrix. For comparing one-dimensional distributions among two samples  $X$  and  $Y$  we use the l1 histogram distance  $D(X, Y) := \frac{1}{2} \sum_i |x_i - y_i|$  where  $x_i$  and  $y_i$  are the empirical probabilities for a given common binning. This distance is upper bounded by 1.

For images, we consider satisfactory validating the results by visual inspection of the samples, since in this case the quality of individual samples is often considered more important than matching the true underlying distribution. We do not use classifier-based metrics such as FID or Inception score since data samples from the original conditioned distribution are not available, hence a comparison is not possible.

In general, the evaluation of the method will depend on the type of dataset.

For our experiments we mostly use score-based generative models based on denoising score matching and SDEs following closely (Song et al. 2021). Conditional generation hyperparameters and more details about models are described in the appendix.

### Wine quality dataset

**Setup.** UCI Wine Quality (Paulo et al. 2009) is a popular dataset composed of two tables, white and red wine, each consisting of 11 real-valued dimensions ( $\mathbb{R}^{11}$ ) and one discrete dimension, the quality, that we discarded. Moreover, we made experiments only with the white wine table. After fitting an unconditional score-based generative model, we generated samples using a constraint based on the following illustrative non-trivial logical formula: (fixed acidity  $\in [5.0, 6.0] \vee$  fixed acidity  $\in [8.0, 9.0]$ )  $\wedge$  alcohol  $\geq 11.0 \wedge$  (residual sugar  $\leq 5.0 \rightarrow$  citric acid  $\geq 0.5$ ).

**Results.** We show in Figure 1 the marginals of the generated samples, compared with samples generated by rejection sampling. There is a high overlap between marginals for most dimensions, and we measured an average l1 distance between correlation coefficients of  $\approx 0.07$ . The largest error, that is associated to one of the dimensions heavily affected by the constraint, is still relatively small. For that con-

straint, the acceptance rate of rejection sampling was only  $\approx 1.67\%$ , meaning that our method samples efficiently in low-probability regions.

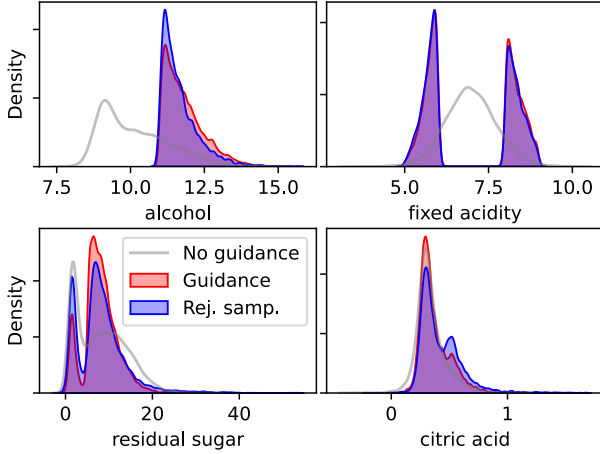


Figure 1: Marginals of white wine data experiment. We generated 5000 samples using our constrained sampling algorithm and as many by rejection sampling. The plot compares the marginals of the dimensions directly involved in the constraint. The last two dimensions are the ones with the largest l1 histogram distance with respect to rejection sampling marginals: 0.15 and 0.13. While the median distance across all dimensions is  $\approx 0.1$ . In order to evaluate the noise of the distance, we also measured the self-distance between two equally sized samples obtained by rejection sampling and observed a median across dimensions of  $\approx 0.05$ .

## MNIST

**Setup.** We test our method also on image datasets in order to investigate the potential in high-dimensional data, although designing meaningful logical constraints for high-dimensional data is harder. We train a model based on a U-net (Ronneberger, Fischer, and Brox 2015) on the MNIST dataset of hand-written digits (LeCun, Cortes, and Burges 2010). Here we demonstrate the application of different constraints:

- *Symmetry*: we impose vertical or horizontal symmetry constraints to generated images, by imposing pixel-by-pixel equality between the image and its symmetrical.
- *Relative filling*: we construct constraints that force the generated image to have more white pixels on a certain part of the image with respect to the remaining. In order to do this, we impose the average pixel value of a given region to be larger than the average pixel value of the remaining pixels by a value of 1.0 (considering normalized images).

**Results.** Our approach seems able to generate images under the constraint of horizontal symmetry (Figure 2), although in many cases ( $\approx 40\%$ ) the generated image did not correspond to an actual digit (even though we also observed  $\approx 10\%$  of non-valid digits in samples generated by



Figure 2: MNIST samples generated imposing a horizontal symmetry constraint.

the unconditional model). Then we show in Figure 3 that we can generate digits that have an imbalance in the number of white pixels in chosen regions.

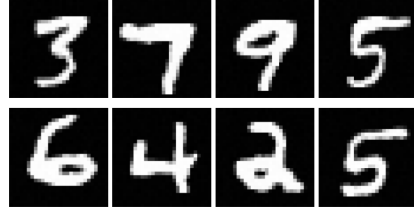


Figure 3: Relative filling experiments. The upper row of digits is generated imposing more white pixels on the upper half than the lower, the lower row is generated imposing more white pixels on the lower half.

In both cases we needed to tune the constraint guidance. In order of decreasing importance, the most influential factors were the logical formula, the constraint intensity ( $k$  or  $\lambda$ ) and the score approximation scheme. In our experiments the tuning mostly consisted in increasing the constraint intensity between runs until a satisfactory trade-off between constraint satisfaction and quality of samples was reached. The success of our method is highly tied to the task. For example, in the image symmetry task the trade-off between samples quality and constraint satisfaction was poorer.

## CelebA

**Setup.** CelebA (Liu et al. 2015) is a popular dataset when demonstrating the capabilities of generative models. We reproduce the setting of (Song and Ermon 2020) where images are resized to 64x64, and use one of their pre-trained (unconditional) score-based models they made available to conduct our experiments. Again we test our method on different constraints:

- *Restoration*: given a differentiable function  $f(\cdot)$ , that represents a corruption process in which information is lost, we define the following constraint:

$$\forall i \ f(\mathbf{x})_i = \tilde{y}_i$$

where  $i$  is the pixel index and  $\tilde{y}$  is a corrupted sample, possibly such that there is a  $\mathbf{y}$  that satisfies  $\forall i \ \tilde{y}_i \approx f(\mathbf{y})_i$ . Such constraint has the effect of sampling possible  $\mathbf{x}$  such that  $\forall i \ f(\mathbf{x})_i = \tilde{y}_i$ , i.e., “inverting”  $f$  or reconstructing the original  $\mathbf{y}$ .  $f$  can be any degradation process, such as downsampling, blurring or adding noise. So our approach can be used for image restoration when the degradation process is known.

- *Color conditioning*: with the objective of controlling the coloring of samples, we use a simple equality constraint between a target RGB color and the mean RGB color of the image.

**Results.** Figure 4 shows how the symmetry soft constraint is successfully met in most samples, and how perfect symmetry is traded-off with realism.



Figure 4: CelebA samples generated imposing a vertical symmetry constraint. Notice the bias for frontal face position and uniform background. While the constraint was useful to improve the symmetry of images, reaching a perfect symmetry by increasing the constraint intensity was not possible without compromising the samples’ quality.

In Figure 5 we show the results of image restoration experiments: for both upsampling and deblurring we corrupted an original image from the dataset, then sampled various images according to the constraints that the downsampled or blurred image should correspond to the original corrupted one. We can see that the samples are realistic and we report a low error with respect to the target corrupted image (the absolute error per channel is approximately less than 0.015).

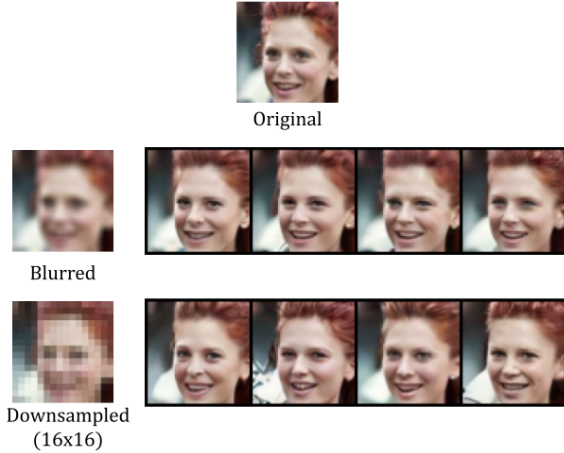


Figure 5: Restoration experiments with CelebA. The image on the top is a sample image from the CelebA dataset. Each row shows samples generated imposing the restoration constraint for different types of corruption processes (Gaussian blurring and downsampling).

Figure 6 shows the result of color conditioning experi-

ments. The resulting samples demonstrate the possibility to manipulate the coloring of an image while preserving the quality of the samples. Nevertheless, it seems the color is excessively manipulated through background, hair, shades or “filter” effect. This is probably due to the naive approach of targeting the mean color.

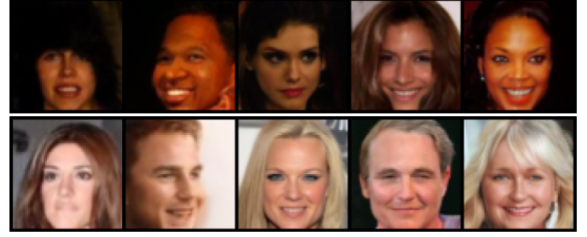


Figure 6: Color conditioning on CelebA. The first row of images is generated imposing the mean color to be equal to a given dark target color, extracted from an image of the dataset. For the second row instead the target was a light color.

Also in this case we found necessary to tune the constraints’ intensity for every task, where in some cases it was necessary in order to regulate the trade-off between sample quality and constraint satisfaction.

### eSIRS surrogate model

**Setup.** A surrogate model is a simplified and efficient representation of a complex, eventually computationally expensive model. It is possible to learn a surrogate model of a complex stochastic dynamical system by fitting a statistical model to a dataset of trajectories observed from it. Following our approach, one can use a score-based generative model to learn an unconditional surrogate model, and then apply constraints to enforce desirable properties. These can be physical constraints the system is known to respect, or features that are rare in unconditioned samples. So we can exploit this method to both assure consistency of trajectories and explore rare (but not necessarily with low density) scenarios. As a case study, we apply our proposed method for the conditional generation of ergodic SIRS (eSIRS) trajectories. The eSIRS model (Kermack, McKendrick, and Walker 1927) is widely used to model the spreading of a disease in an open population<sup>3</sup>. The model assumes a fixed population of size  $N$  composed of Susceptible ( $S$ ), Infected ( $I$ ), and Recovered ( $R$ ) individuals. We consider trajectories with  $H$  discretized time steps, thus we have that the sample space is  $\mathcal{X}_{\text{eSIRS}} := (\mathbb{N}_0^2)^H$ , where the two dimensions are  $S$  and  $I$  ( $R$  is implicit since  $R = N - S - I$ ).

First we train a score-based generative model to fit trajectories that were generated by a simulator, with  $H = 30$  and  $N = 100$ . Then we experimented with the application of different constraints, including the following consistency constraints:

<sup>3</sup>Open in the sense of having infective contacts with external individuals, not part of the modelled population.



- *Non-negative populations*:  $\forall t S(t) \geq 0 \wedge I(t) \geq 0$
- *Constant population*:  $\forall t S(t) + I(t) \leq N$

**Results.** We show in Figure 7 and Figure 8 two experiments with two different constraints. In both experiments the consistency constraints (positive and constant population) were always met, with a small improvement over the unconditional model. In the two experiments we additionally imposed a bridging constraint and an inequality, that were also met with minimal error.

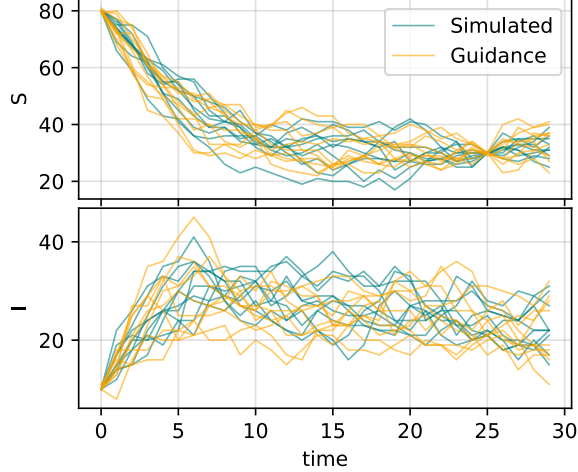


Figure 7: Bridging with eSIRS time series. We show here a subsample of the 5000 time series generated with constraint guidance (orange) with a subsample of the  $> 50000$  time series generated by rejection sampling from the simulator (green). Additionally to the consistency constraints, that are always met, we imposed the following equalities:  $S(0) = 95$ ,  $I(0) = 5$ ,  $S(25) = 30$ . Constraints are generally met: the average l1 absolute difference with all three target values is below 0.19. The l1 histogram distance for each time step marginal is relatively small, considering that it accounts also for the error of the unconditional model: for  $S$  and  $I$  the median l1 histogram distance across time are  $\approx 0.11$  and  $\approx 0.13$ . The median self distance across time between two samples of 5000 instances of rejection sampling was  $\approx 0.04$  for both  $S$  and  $I$ .

## Related Work

Controllable generation with score-based models is discussed in (Song et al. 2021), where they both treat the case when the noise conditional classifier  $p_t(\mathbf{y}|\tilde{\mathbf{x}})$  can be trained and when it is not available. In that case, a method for obtaining such an estimate without the need of training auxiliary models is discussed and applied to conditional generation tasks such as inpainting and colorization. Still, the estimate is applicable only assuming the possibility to define  $\mathbf{y}_t$  such that  $p(\mathbf{y}_t|\mathbf{y})$  and  $p(\mathbf{x}_t|\mathbf{y}_t)$  are tractable. In (Sohl-Dickstein et al. 2015) they suggest a method to sample from the product of a distribution learned with a diffusion model  $p(\mathbf{x})$  and a given distribution or bounded positive function

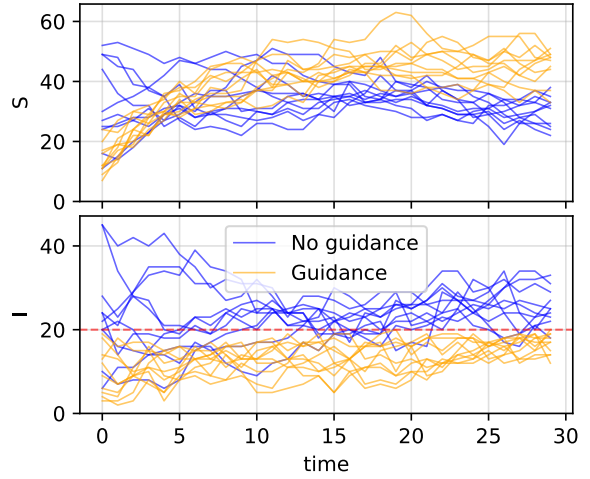


Figure 8: Imposing an inequality on eSIRS time series. We show here a subsample of the 100 time series generated with and without constraint guidance. Additionally to the consistency constraints, that are always met, we imposed  $\forall t I(t) \leq 20$ , that is perfectly met in 99% of the samples.

$r(\mathbf{x})$ . The method consists in modifying the reverse diffusion process by multiplying the reverse kernels  $q(\mathbf{x}_{t-1}|\mathbf{x}_t)$  by  $r(\mathbf{x})$ , using an approximation when this cannot be done analytically. In practice they apply this method only to the particular case of inpainting, that is easily solvable with heuristics. Earlier works explored the combination of unconditional latent variables generative models such as Generative Adversarial Networks (GANs) (Goodfellow et al. 2014) or Variational Autoencoders (VAEs) (Kingma and Welling 2013) with constraints to produce conditional samples (Engel, Hoffman, and Roberts 2017). As for DDPMs (denoising diffusion probabilistic models), recent research has focused on leveraging pre-trained unconditional models as priors for solving inverse problems as in (Kadkhodaie and Simoncelli 2021) where they use DDPMs for solving linear inverse imaging problems, and (Graikos et al. 2022), (Bansal et al. 2023) where they generalize to a generic guidance.

## Conclusion

We have shown how we can exploit unconditional score-based generative models to sample under user-defined logical constraints, without the need for additional training. Our experiments demonstrate the effectiveness in several contexts, such as tabular and high-dimensional data. Nevertheless, the conditional score approximation often needs tuning, and the error with respect to the true target distribution can be substantial, especially for multi-modal distributions, where Langevin Monte Carlo struggles to explore all the modes. For images, we had to trade-off between sample quality and constraint satisfaction. Future work will focus on finding better approximation schemes, borrowing ideas from recent works that focused on general guidance for images (Bansal et al. 2023; Graikos et al. 2022).

## References

- Badreddine, S.; d'Avila Garcez, A. S.; Serafini, L.; and Spranger, M. 2020. Logic Tensor Networks. *CoRR*, abs/2012.13635.
- Badreddine, S.; Serafini, L.; and Spranger, M. 2023. logLTN: Differentiable Fuzzy Logic in the Logarithm Space. *ArXiv*, abs/2306.14546.
- Bansal, A.; Chu, H.-M.; Schwarzschild, A.; Sengupta, S.; Goldblum, M.; Geiping, J.; and Goldstein, T. 2023. Universal guidance for diffusion models. In *Proceedings of the IEEE/CVF Conference on Computer Vision and Pattern Recognition*, 843–852.
- Dhariwal, P.; and Nichol, A. 2021. Diffusion models beat gans on image synthesis. *Advances in Neural Information Processing Systems*, 34: 8780–8794.
- Engel, J.; Hoffman, M.; and Roberts, A. 2017. Latent constraints: Learning to generate conditionally from unconditional generative models. *arXiv preprint arXiv:1711.05772*.
- Ganchev, K.; Graça, J.; Gillenwater, J.; and Taskar, B. 2010. Posterior regularization for structured latent variable models. *The Journal of Machine Learning Research*, 11: 2001–2049.
- Goodfellow, I.; Pouget-Abadie, J.; Mirza, M.; Xu, B.; Warde-Farley, D.; Ozair, S.; Courville, A.; and Bengio, Y. 2014. Generative adversarial nets. *Advances in neural information processing systems*, 27.
- Graikos, A.; Malkin, N.; Jovic, N.; and Samaras, D. 2022. Diffusion models as plug-and-play priors. *Advances in Neural Information Processing Systems*, 35: 14715–14728.
- Ho, J.; Jain, A.; and Abbeel, P. 2020. Denoising diffusion probabilistic models. *Advances in neural information processing systems*, 33: 6840–6851.
- Hu, Z.; Yang, Z.; Salakhutdinov, R. R.; Qin, L.; Liang, X.; Dong, H.; and Xing, E. P. 2018. Deep generative models with learnable knowledge constraints. *Advances in Neural Information Processing Systems*, 31.
- Hyvärinen, A.; and Dayan, P. 2005. Estimation of non-normalized statistical models by score matching. *Journal of Machine Learning Research*, 6(4).
- Kadkhodaie, Z.; and Simoncelli, E. 2021. Stochastic solutions for linear inverse problems using the prior implicit in a denoiser. *Advances in Neural Information Processing Systems*, 34: 13242–13254.
- Kermack, W. O.; McKendrick, A. G.; and Walker, G. T. 1927. A contribution to the mathematical theory of epidemics.
- Kingma, D. P.; and Welling, M. 2013. Auto-encoding variational bayes. *arXiv preprint arXiv:1312.6114*.
- LeCun, Y.; Cortes, C.; and Burges, C. 2010. MNIST handwritten digit database. *ATT Labs [Online]*. Available: <http://yann.lecun.com/exdb/mnist>, 2.
- Liu, Z.; Luo, P.; Wang, X.; and Tang, X. 2015. Deep learning face attributes in the wild. In *Proceedings of the IEEE international conference on computer vision*, 3730–3738.
- Parisi, G. 1981. Correlation functions and computer simulations. *Nuclear Physics B*, 180(3): 378–384.
- Paulo, C.; A., C.; F., A.; T., M.; and J., R. 2009. Wine Quality. UCI Machine Learning Repository. DOI: <https://doi.org/10.24432/C56S3T>.
- Rombach, R.; Blattmann, A.; Lorenz, D.; Esser, P.; and Ommer, B. 2022. High-resolution image synthesis with latent diffusion models. In *Proceedings of the IEEE/CVF conference on computer vision and pattern recognition*, 10684–10695.
- Ronneberger, O.; Fischer, P.; and Brox, T. 2015. U-net: Convolutional networks for biomedical image segmentation. In *Medical Image Computing and Computer-Assisted Intervention—MICCAI 2015: 18th International Conference, Munich, Germany, October 5-9, 2015, Proceedings, Part III 18*, 234–241. Springer.
- Sohl-Dickstein, J.; Weiss, E. A.; Maheswaranathan, N.; and Ganguli, S. 2015. Deep Unsupervised Learning using Nonequilibrium Thermodynamics. *CoRR*, abs/1503.03585.
- Song, Y.; and Ermon, S. 2019. Generative modeling by estimating gradients of the data distribution. *Advances in neural information processing systems*, 32.
- Song, Y.; and Ermon, S. 2020. Improved techniques for training score-based generative models. *Advances in neural information processing systems*, 33: 12438–12448.
- Song, Y.; Garg, S.; Shi, J.; and Ermon, S. 2020. Sliced score matching: A scalable approach to density and score estimation. In *Uncertainty in Artificial Intelligence*, 574–584. PMLR.
- Song, Y.; Sohl-Dickstein, J.; Kingma, D. P.; Kumar, A.; Ermon, S.; and Poole, B. 2021. Score-Based Generative Modeling through Stochastic Differential Equations. In *International Conference on Learning Representations*.
- van Krieken, E.; Acar, E.; and van Harmelen, F. 2022. Analyzing differentiable fuzzy logic operators. *Artificial Intelligence*, 302: 103602.
- Vincent, P. 2011. A connection between score matching and denoising autoencoders. *Neural computation*, 23(7): 1661–1674.



## Appendix

### Unconditional models

For all datasets except CelebA we trained unconditional generative models from scratch. We used score based generative models based on SDEs (Song et al. 2021), also following many of the implementation details of the repository of the original paper. We used two types of SDEs in our experiments: the variance exploding SDE (VE) and a variant of the variance preserving SDE, the sub-VP SDE. As score-matching algorithm we mostly used denoising score-matching and experimented also with sliced score matching. As numerical solver of the reverse SDE we used Euler-Maruyama, the simplest method. For most of our experiments with SDE we used predictor-corrector sampling, i.e., adding steps of Langevin dynamics after each step of reverse SDE solving. As discussed previously we often performed additional Langevin MCMC steps at  $t = 0$ . For the experiments with celebA we used a pre-trained model made available in the repository relative to (Song and Ermon 2020), that is based on annealed Langevin dynamics. For tabular data and time series the neural network architectures we used were simple multi layer perceptrons. More complete information can be found in the code repository that we made available.

### Training a score model for tabular data

In (Song and Ermon 2020) they suggest scaling the neural network approximating the noise dependent score in the following way:  $s_\theta(\mathbf{x}, t) = \frac{\mathbf{f}_\theta(\mathbf{x})}{\sigma_t}$  where  $\mathbf{f}_\theta(\mathbf{x})$  is the neural network and  $\sigma_t$  is the standard deviation of the diffusion kernel  $q(\tilde{\mathbf{x}}|\mathbf{x})$ . The issue is that when  $t \approx 0$ ,  $\sigma_t$  will approach zero and the score will explode. Apparently this is not an issue for image datasets, where modelling the exact distribution is less important than the quality of samples. This is not the case for time series and tabular data, where we are interested in correctly modelling the noisy distribution that generated the data. Moreover this is particularly important when we perform Langevin MCMC at  $t \approx 0$  in order to exploit the knowledge of the exact conditional score. We then elaborated some practices in order to improve the estimate in these domains:

- We capped the scaling factor  $\sigma_t^{-1}$  by a certain limited value. This value has to be an hyperparameter of the training.
- We used large batch sizes and occasionally accumulated the gradient across several batches before performing the weights update. This helps reducing the noise of the score-matching loss for low values of  $\sigma_t$ .
- We occasionally used sliced score matching to learn the noise dependent score on data corrupted by the diffusion process, also in combination with denoising score matching. The reason is that we found the sliced score matching loss to be less noisy than the denoising score matching loss.

### Normalization

Data in experiments was normalized. Since the constraint is defined in the original data space, one has to take the normalization into account when applying the constraint to transformed data. Given a data point  $\mathbf{x}$ , a differentiable and invertible transformation  $\mathbf{f}(\mathbf{x})$  and the constraint  $c_x(\mathbf{x})$ , the actual constraint that is applied to transformed data points  $\mathbf{y} = \mathbf{f}(\mathbf{x})$  is  $c_y(\mathbf{y}) = c_x(\mathbf{f}^{-1}(\mathbf{x}))$ .

### Constrained generation settings

In Table 2 are shown hyperparameters that are used in the constrained generation experiments. In experiments that involved equality constraints, we specify which function we used: LPL (log-probabilistic logic) refers to the first definition we gave in Table 1, otherwise we used the squared error. We also indicate the values of  $k$  and  $\lambda$  we used to regulate the constraints' intensity. The step size for Langevin MCMC was chosen dynamically depending on the norm of the score, we used the same implementation as in (Song et al. 2021). Constraints' intensity was chosen by hand, monitoring the trade-off between constraint satisfaction and samples quality across multiple experiments. The score approximation strategy ( $g(t)$ ) was less influential than the constraint intensity, although we generally observed slightly better performances for SNR. For the white wine experiment, we observed instead the linear approximation to perform slightly better.

### Hardware specifications

We run the experiments that involved less computational power (tabular data and time series) on a machine with the following hardware specifications:

- Processor: Intel® Core™ i5-7200U CPU @ 2.50GHz × 4
- Memory: 8 GiB

Instead we run experiments involving images on a machine with the following hardware specifications:

- Processor: AMD Ryzen Threadripper 2950X 16-Core Processor
- Memory: 125 GiB
- GPU: NVIDIA RTX A5000

Table 2: Constrained generation details

<b>Experiment</b>	<b>Constraint</b>	<b><math>g(t)</math></b>	<b>Langevin MCMC steps</b>
Toy example	LPL( $k = 50$ )	SNR	200
White wine	LPL( $k = 50$ )	Linear	4000
eSIRS bridging	LPL, equality: $k = 7$ consistency: $k = 1$	SNR	2000
eSIRS inequality	LPL, inequality: $k = 25$ consistency: $k = 1$	SNR	2500
MNIST relative filling	LPL( $k = 80$ )	SNR	20
MNIST inpainting	Squared error ( $\lambda = 1$ )	Linear	0
MNIST symmetry	LPL( $k = 5$ )	SNR	0
CelebA symmetry	Squared error ( $\lambda = 0.19$ )	SNR	0
CelebA color conditioning	Squared error, light: $\lambda = 1000$ dark: $\lambda = 800$	SNR	0
CelebA restoration	Squared error, deblurring: $\lambda = 100$ upsampling: $\lambda = 600$	SNR	0

Column	l1 histogram distance
Fixed Acidity	0.049
Volatile Acidity	0.052
Citric Acid	0.13
Residual Sugar	0.15
Chlorides	0.077
Free Sulfur Dioxide	0.094
Total Sulfur Dioxide	0.11
Density	0.10
pH	0.087
Sulphates	0.12
Alcohol	0.11

Table 3: White wine experiment: l1 histogram distance for different columns. This table compares the marginal distributions of the 5000 samples generated with constraint guidance with the same number of samples generated with rejection sampling. The median across-dimensions of the measured self distance between two distinct samples of 5000 instances generated by rejection sampling was of  $\approx 0.05$

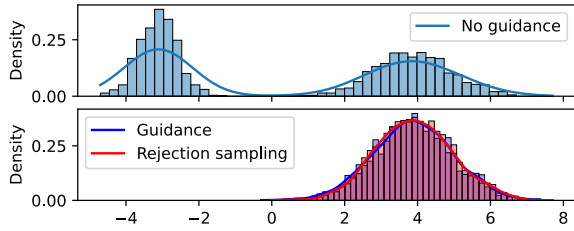


Figure 9: Constraint guidance on a toy dataset. We fitted a score-based generative model on data generated according to a mixture of two Gaussian distributions  $\mathcal{N}(\mu = -3, \sigma = 0.5)$ ,  $\mathcal{N}(\mu = 4, \sigma = 1)$  with equal mixing coefficients. Given the constraint  $x \geq 0$ , our method generates samples that are not distinguishable from ones generated with rejection sampling. We also show the generated distribution without guidance.



Figure 10: Inpainting on MNIST. The first image on the left shows a digit with the masked pixels in yellow. The other images are generated imposing the inpainting constraint, that consists in a pixel-by-pixel equality of the unmasked pixels of the original image.